Journal of Molecular Graphics and Modelling 59 (2015) 21–30

Contents lists available at ScienceDirect

Journal of Molecular Graphics and Modelling

journal homepage: www.elsevier.com/locate/JMGM

Configurational study of amino-functionalized silica surfaces: A density functional theory modeling

Samira Hozhabr Araghi [a], Mohammad H. Entezari [a,b,*], Mohammad Sadegh Sadeghi Googheri [c]

[a] Sonochemical Research Center, Department of Chemistry, Ferdowsi University of Mashhad, 91775 Mashhad, Iran
[b] Environmental Chemistry Research Center, Department of Chemistry, Ferdowsi University of Mashhad, 91775, Mashhad, Iran
[c] Biophysical Chemistry Laboratory, Department of Chemistry, Ferdowsi University of Mashhad, 91775 Mashhad, Iran

ARTICLE INFO

Article history:
Received 3 January 2015
Received in revised form 18 February 2015
Accepted 26 March 2015
Available online 3 April 2015

Keywords:
Amino-functionalized silica
APTES
Hydrolyzed forms
DFT
NBO
AIM

ABSTRACT

Despite extensive studies of the amino-functionalized silica surfaces, a comprehensive investigation of the effects of configuration and hydrolysis of 3-aminopropyltriethoxysilan (APTES) molecules attached on silica has not been studied yet. Therefore, the methods of quantum mechanics were used for the study of configuration and hydrolysis forms of APTES molecules attached on the surface. For this purpose, five different categories based on the number of hydrolyzed ethoxy groups including 16 configurations were designed and analyzed by the density functional theory (DFT) method. The steric hindrance as an effective factor on the stability order was extracted from structural analysis. Other impressive parameters such as the effects of hydrogen bond and electron delocalization energy were obtained by using the atoms in molecules (AIM) and natural bond orbitals (NBO) theories.

Consequently, it was found that the stability of configurations was attributed to steric effects, hydrogen bond numbers and electron delocalization energy. The maximum stability was achieved when at least two of these parameters cooperate with each other.

1. Introduction

Nanoparticles have been intensively researched during the last few decades. Due to their high surface to volume ratio, the nanoparticles have unique properties than bulk materials [1]. Silica nanoparticles (NPs) is perhaps one of the most studied materials in nanoscience. This is due to the remarkable properties such as high chemical and thermal stability and its possibility to be modified by a wide range of functional groups [2]. Modification of silica surfaces with variety of functional groups such as thiol [3], amine [4,5], phenyl [6] was performed with different kinds of organosilanes. APTES is most frequently used as organosilane agent for preparation of amino-functionalized silica surfaces [7]. Aminosilylated surfaces are widely used in biochemistry [8], catalyst technology [9], analytical chemistry [10] and industries [11]. Functionalized surfaces can be prepared in the gas or liquid phases [12]. But, the modification of silica surfaces with different types of organosilanes is frequently achieved in liquid phase that includes the sol–gel, aqueous and organic solvent methods [11]. APTES forms an internal zwitterion in water while anhydrous organic solvent produces a uniform monolayer of APTES on the surface [13]. The presence of small amount of water in anhydrous organic solvent, for example toluene, has an important effect on the mechanism of molecular layer formation and structure of the deposited layer of organosilanes [14]. Silanization that is most frequently used to attach APTES molecules on different silica surfaces begins with the hydrolysis of ethoxy groups in APTES. This step catalyzes by the presence of water molecules and leads to the formation of silanols. The condensation of APTES silanols with silanol groups present on silica surface (surface silanols) results in the formation of a monolayer of APTES via siloxane bonds (Si—O—Si). In addition, there are other possible ways for interaction of APTES with surface silanols and/or adjacent APTES via hydrogen bonding or electrostatic attraction. These interactions reduce the number of available silanol groups on silica surface and APTES for more formation of siloxane bond [15,16].

The attached APTES layer on silica surfaces have been characterized by many techniques including Fourier transform infrared spectroscopy (FTIR) [17], thermogravimetric analysis (TGA) [18], CHN elemental analysis [4], and ellipsometry [19]. But, these methods are unable to determine the numbers of hydrolyzed ethoxy

* Corresponding author at: Sonochemical Research Center, Environmental Chemistry Research Center, Department of Chemistry, Ferdowsi University of Mashhad, 91775 Mashhad, Iran. Tel.: +98 9153114320; fax: +98 511 8795457.
E-mail address: moh_entezari@yahoo.com (M.H. Entezari).

http://dx.doi.org/10.1016/j.jmgm.2015.03.006
1093-3263/

groups on the silica surfaces. Therefore, use of the quantum mechanics methods can be useful for this purpose. Application of computational chemistry cover an extremely wide range from predicting the structure, configuration stability, spectra (IR, NMR or UV–vis) and reactivity of complicated molecules to understanding the catalytic property of materials [20]. Quantum mechanics calculations such as ab-initio [21], DFT [22] and combination methods [23] were used as an extensive branch of computational chemistry for determination of stability and surface adsorption on silica surfaces [24]. Unfortunately, high accuracy quantum mechanical methods cannot be used for the large molecules. The ONIOM method which is originally developed by Morokuma and coworkers [25] is among the modern proposals devoted to tackle large molecular systems with quantum mechanical methods.

In the present work, for the first time a theoretical calculation on possible configurations of amino-functionalized silica surfaces were performed by ONIOM method. For this purpose, a silica surface was designed and silanol density for this surface was considered as 6 OH per nm^2. Two APTES molecules were anchored on it in the energetically favorable configuration. Additionally four water molecules were placed on the top of surface for designing the hydrolyzed configurations. Based on the number and position of hydrolyzed ethoxy groups, 16 different configurations were constructed and optimized in the best available and applicable level of theory. Finally, for better understanding of effective factors on the stability order of configurations, the natural bond orbital (NBO) [26] and atoms in molecules (AIM) [27] were performed on the system.

2. Materials and methods

The first step in our calculation was the design of the silica surface. It was modeled similar to other works [28,29]. Based on Niinisto et al. study [30], the number of hydroxyl groups on the surface (silanol groups) were dedicated to 6 groups. To make simpler, in our calculation a mono layer surface was selected and the inner sheets were replaced by frozen methyl groups to keep crystalline surface structure (Fig. 1). This structure was optimized at the B3LYP/SDD level of theory and was considered as the initial construction for further calculations.

After designing the initial surface, APTES molecules were added on the surface to form the amino-functionalized silica surface. Because of APTES molecule size and its steric hindrance, only two molecules can be attached to 1 $nm^2$of the surface. Our initial calculations revealed that the best position for these two molecules was achieved by replacing the H_{38} and H_{32} (Fig. 1). Since four hydrolysable ethoxy groups were on the surface, four water molecules were placed on it to simulate the hydrolyzed forms. The proposed amino-functionalized silica surface included 153 atoms, which was costly and time-consuming for high-level quantum mechanical calculations. Hence, a two-layer ONIOM method [25] was used for optimization the designed surface. Here 86 atoms include four silanols, two functionalized silanols, two anchored APTES groups and four water molecules were assigned to the high layer, quantum mechanics (QM), and other 67 atoms were belonged to the low layer, molecular mechanic (MM) (Fig. 2). The QM subunit was optimized by the DFT methods via using the B3, Becke three parameters [31], for exchange functional and PW91, Perdew–Wang 91 [32], for non-local correlation corrections with applying the 6–31 g (d) basis sets [33]. But the MM layer uses the universal force filed (UFF) [34] for optimization. This initial amino-functionalized silica called as 4-ethoxy that none of ethoxy groups is hydrolyzed.

As can be seen from Fig. 2, water molecules can hydrolyze the attached groups in APTES. Depends on the number of hydrolysable groups (e.g. OCH_2CH_3), there are four hydrolyzed categories. If one of the ethoxy groups is replaced by hydroxyl group, the 3-ethoxy category will be formed. This reaction could be continued until all of the ethoxy groups will be substituted and a fully hydrolyzed surface will be produced. It is clear that the 2-ethoxy, 1-ethoxy and 0-ethoxy categories are generated by progress the reaction (Scheme 1). Each category has different forms depending on the location of the hydrolyzed group. Since in 0-ethoxy and 4-ethoxy categories all and none of ethoxy groups are hydrolyzed respectively, they have only one form. In the 3-ethoxy classification, one group is hydrolyzed and due to four possible hydrolysable positions, it has four different forms. There are similar conditions for 1-ethoxy that one unhydrolyzed ethoxy group could be existed in the four various forms. Between these categories, the 2-ethoxy has most forms, six forms, because of its two ethoxy groups are hydrolyzed simultaneously. Therefore based on our calculations, when the hydrolysis reaction is happened on the surface, 16 possible forms are existed per 1 nm^2. The other forms (15) were optimized at the same level of theory as 4-ethoxy form.

For increasing the accuracy of energy results, the single point energy calculations were performed at the level of B3PW91:6-311++G (d, p: UFF). Furthermore, the solvent effects was considered by SCRF = CPCM (solvent = hexane) keyword which performs a PCM calculation [35] using the CPCM polarizable conductor calculation model [36]. All calculations were performed by using Gaussian 09 program package [37].

Finally, the nature of effective surface interactions in the most stable configurations was realized with NBO and AIM analyses. For this purpose, the most stable form of each category was selected and additional inspections were done on them. NBO analysis has been used with the purpose of understanding and describing electron delocalization and hydrogen bond (HB). Delocalization of electron density between occupied Lewis type and unoccupied non-Lewis orbitals corresponds to a stabilizing donor–acceptor interaction. The energy of these interactions can be computed by the NBO calculations, which come from the second order perturbation theory. In addition, the type and strength of the hydrogen bonds can be determined from charge transfers (CT) between involved NBO orbitals and their energies. Also AIM theory as a powerful method are applied for investigation the molecule's structure and bonding. This theory is based on topological analysis of the electron charge density (ρ). Electron density properties at bond critical point (BCP) are used for description of bond formation in AIM theory. Two most important parameters in this theory are bond critical point charge density (ρ_{BCP}) and the Laplacian of charge density ($\nabla^2\rho_{BCP}$), which are used for description of the strength and type of bond. For a localized bond, covalent bond, the ρ_{BCP} and $\nabla^2\rho_{BCP}$ have positive and negative values respectively while for a delocalized bond, such as hydrogen bonds, both of them are positive with lower values [38].

The NBO calculations were carried out on the B3PW91/6-311++G (d, p) level of theory in hexane environment by using the NBO package included in Gaussian 09 program [39]. Moreover, the electron density and the type of existing bond on the surface of different forms were investigated by AIM theory by means of AIM All 2010 program package [40]. It is mentioned that the QM level was used for AIM and NBO computations.

3. Results and discussion

3.1. Structural and energy analysis

As it was mentioned, the starting structure for our purpose was the 4-etoxhy form which its surface was not hydrolyzed (Fig. 3). Due to the positional similarity of 1, 3 and 5 surface silanols and

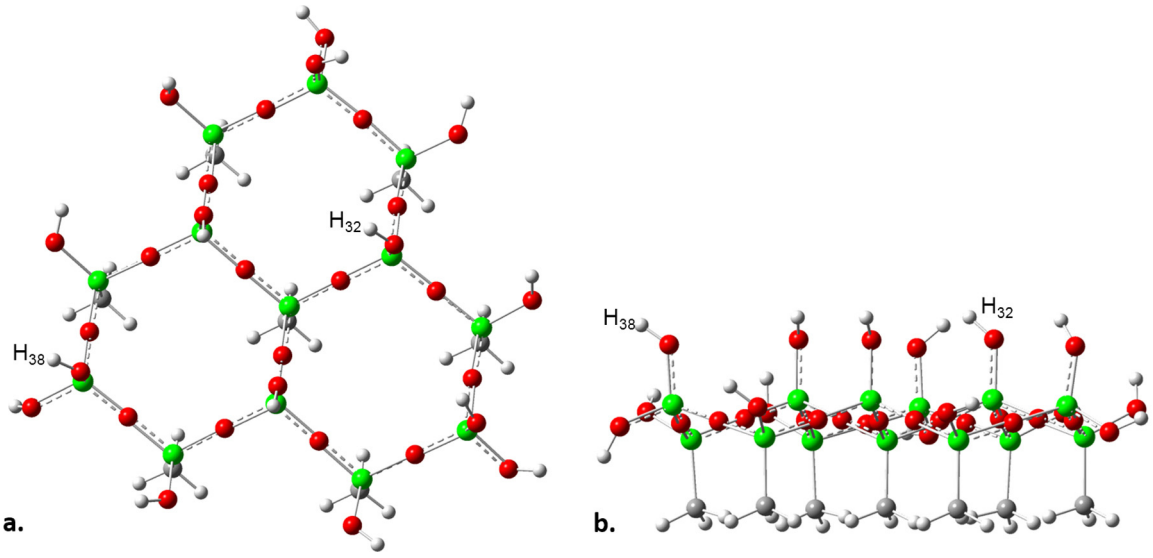

Fig. 1. The optimized silica surface structure from (a) top and (b) side view. In the side view, the outer and inner layers are revealed obviously. H_{38} and H_{32} are demonstrated as the proper positions for the substitution of APTES groups. The oxygen, carbon, silicon and hydrogen atoms are shown as red, gray, green and white color, respectively. (For interpretation of the references to color in this figure legend, the reader is referred to the web version of this article.)

steric hindrances between 2, 4 and 6 situations, the best configuration for locating APTES molecules was on the surface silanols of 1 and 4. The structural analysis shows that the orientation of the surface silanols, attached APTES and water molecules optimize the repulsion and attraction forces on the silica surface. It seems that the most important interactions on the functionalized silica surface are HBs and spatial interactions. The depth investigation of optimized surface shows that the surface silanols, ethoxy groups and amine groups have high potential to form HB with each other and water molecules. Assigned bond length in Table 3, between mentioned groups, are in the range of HB. Apparently, orientations of water molecules are such that the maximum numbers of HBs are formed. We guess that another HB could be formed between amine group of $APTES_2$ and oxygen atom of SiI_3.

Besides HBs, the steric hindrances of bulky ethoxy groups play an important role in the arrangement of functional groups on the silica surface. Ethoxy groups exert repulsive force that leads to orient away each other and the surface. This causes that the angles of surface siloxane bonds turn from bent to linear for decreasing the repulsive forces. Due to the changes in the angle, the amine groups of attached APTES molecules can interact with the surface (Fig. 3b). It is expected, when the hydrolysis is occurred and a smaller hydroxyl group is replaced, the steric effects decrease and the orientation of attached APTES molecules alter too.

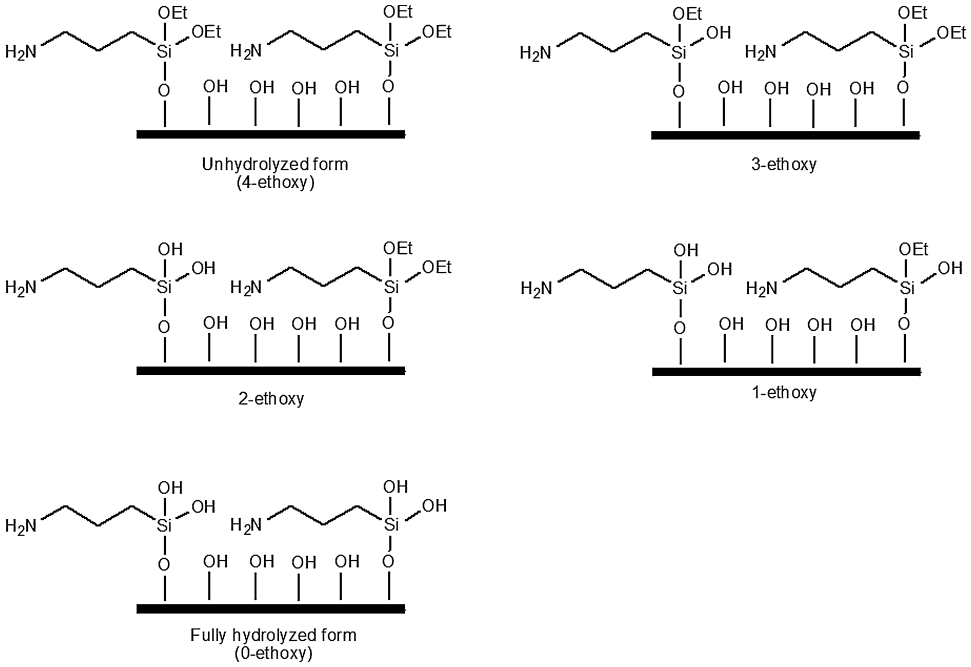

Scheme 1. Schematic representation of five possible categories of amino-functionalized silica surface. 4-ethoxy category has one form, 3-ethoxy and 1-ethoxy have four forms, while the 2-ethoxy and 0-ethoxy have six and one forms, respectively.

Table 1
Relative energy of different forms for amino-functionalized silica surface in kcal mol^{-1}. The 4-ethoxy surface was selected as the reference configuration.

Category	Form	Relative energy
4-ethoxy	4-ethoxy	0.00
3-ethoxy	3-ethoxy1	−8.4
	3-ethoxy2	−0.8
	3-ethoxy3	−7.0
	3-ethoxy4	−13.4
2-ethoxy	2-ethoxy1	−8.4
	2-ethoxy2	−15.3
	2-ethoxy3	−21.2
	2-ethoxy4	−7.8
	2-ethoxy5	−17.3
	2-ethoxy6	−19.1
1-ethoxy	1-ethoxy1	−22.8
	1-ethoxy2	−30.4
	1-ethoxy3	−13.2
	1-ethoxy4	−15.4
0-ethoxy	0-ethoxy	−18.6

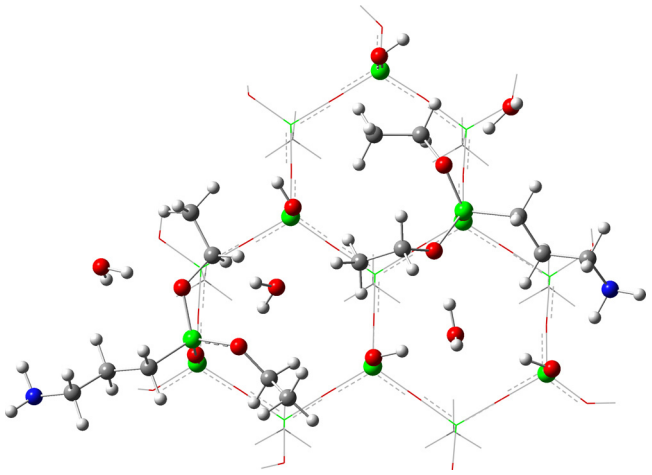

Fig. 2. Bi-layer structure for amino-functionalized silica surface. The high and low layers are shown as ball and bond type and wireframe, respectively. The nitrogen atoms are displayed as blue ball.

When the hydrolysis reaction is happened and one ethoxy group is replaced with hydroxyl group, different configurations of 3-ethoxy surface are formed. If the OEt_1 is hydrolyzed, the 3-ethoxy1 will be made and 3-ethoxy2, 3-ethoxy3 and 3-ethoxy4 forms are produced by hydrolysis of ethoxy groups OEt_2, OEt_3, OEt_4, respectively. Fig. 4 shows the optimized structures of these forms. Comparison these structures with 4-ethoxy indicates that the type of interactions is similar with three forms of 3-ethoxy except where the substitution is occurred. Because of this exchange, the strain on the surface is decreased and configurations become more stable, which can see from Table 1. However, the story of 3-ethoxy4 is different. In this form, the W_3 transfers to the hydrolyzed location and causes to form a HB network (Fig. 4, 3-ethoxy4). It appears that this additional factor leads to an extra stability, about two times, for this form with respect to other forms in this category (see Table 1).

There are different positions for hydrolysis of second group. Therefore, the numbers of the forms for 2-ethoxy are more than other categories. In 2-ethoxy1, geminal ethoxy molecules are replaced by two hydroxyl groups while for the 2-ethoxy2 the exchanged groups are vicinal ethoxy groups namely OEt_1 and OEt_3. Additionally, against substitution of ethoxy groups led to 2-ethoxy3 form. The same procedure was used for designing the three other forms for this category (Fig. 5). Structural analysis confirms that the number of HB has important role in the order of stability for these forms. The number of HBs is estimated 8 for 2-ethoxy1 and 2-ethoxy4 forms while it is nine for 2-ethoxy2. It appears that this disparity leads to the more stability of 2-ethoxy2 with respect to 2-ethoxy1 and 2-ethoxy4 forms. In the more stable configurations in this category in addition to existence of 10 (2-ethoxy5 and 2-ethoxy6 forms) and 11 (2-ethoxy3) HBs, a HB network is shaped on the surface. Table 1 illustrates that with exchanging the second ethoxy group the relative energies of this category decline. This stems from the fact that this substituting increases the number of HB and decreases the steric effects.

By hydrolysis reaction progress and replacing of third ethoxy group, 1-ethoxy category is formed. Nomenclature of this category forms is done based on unhydrolyzed ethoxy position. Four optimized configurations of this group are displayed in Fig. 6. Deep analysis of optimized structure indicates that an extensive HB network take places in the 1-ethoxy1 and 2 configurations. But in other forms, the position of functional groups on the surfaces is such that the HB network could not be formed. Because of this dissimilarity, an energy difference is created between them (Table 1).

The last possible form for our surface is the 0-ethoxy state that all ethoxy groups are hydrolyzed in APTES molecules. Our calculations

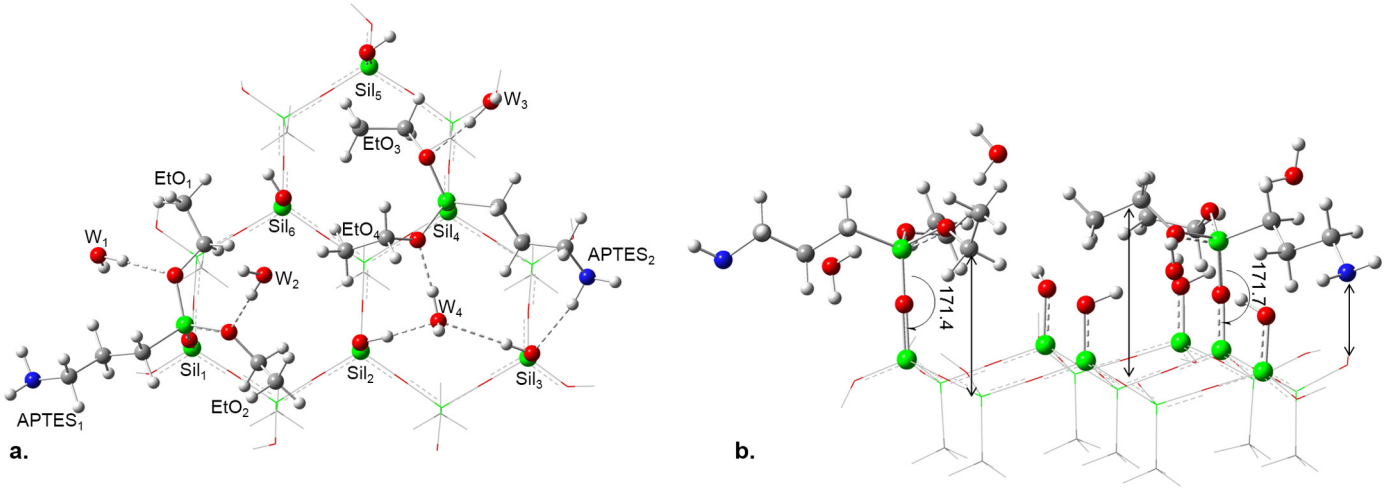

Fig. 3. (a) Top view of the optimized structure of 4-ethoxy form. The surface silanol groups, water molecules and ethoxy groups in $APTES_1$ and $APTES_2$ are detected as Sil_1 to Sil_6, W_1 to W_4 and EtO_1 to EtO_4, respectively. (b) Angles of Si—O—Si are displayed in degree in side view. The distance between functional groups and surface are presented with arrow.

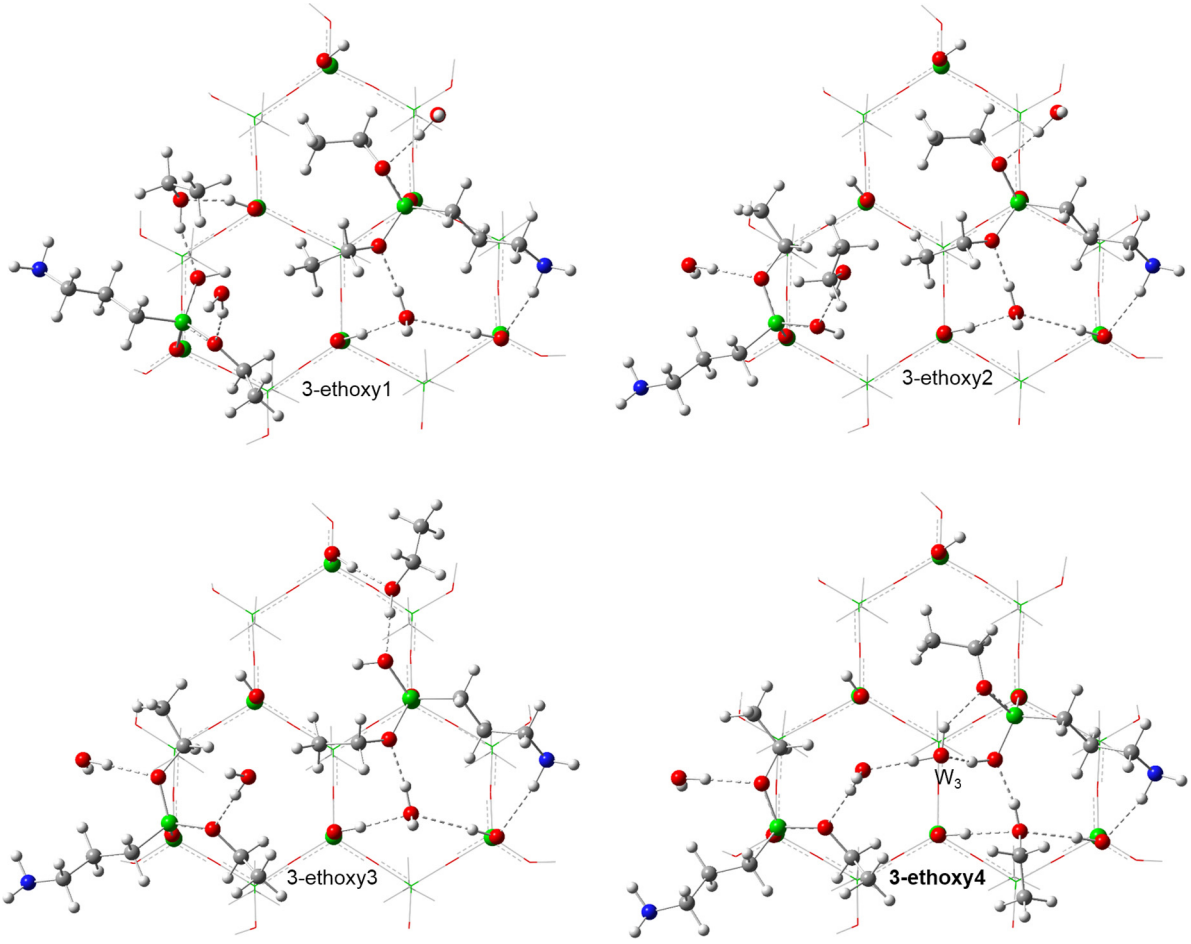

Fig. 4. Optimized structures of 3-ethoxy category forms. HB network in the 3-ethoxy4 form is displayed as dash lines. W_3 stands for water molecule NO.3.

show that unlike other forms, the amine group of the $APTES_2$ in this form is orientated away from silica surface. As a result the HB between this group and the Sil_3does not form. It seems that with the hydrolysis of all ethoxy groups the steric effects on the surface reduce and two siloxane angles become more bent. Therefore, two new HBs are formed, which did not exist on the other forms (Fig. 7).

3.2. Evaluation of effective parameters in stability order

After analysis of optimized structures, it is necessary to evaluate the efficient causes of different relative energies. Therefore, herein five forms including the most stable configure of each category were selected for more investigations.

As it was mentioned, the first factor that can be concluded from structural analysis was the steric hindrance. The detailed analysis of relative energies indicates that there is a proper relation between the energy and the numbers of hydrolyzed ethoxy (HEtO) groups (Table 2). As Fig. 8a shows the relative energy decreases with increasing the number of HEtO groups from 4-ethoxy to 1-ethoxy. It seems that the replacing of bulky ethoxy groups with smaller hydroxyl groups during the hydrolysis reaction decreases the steric hindrances and increases the stability. But in the case of 0-ethoxy, the stability decreases despite above procedure that this inconsistency may be due to the effect of other factors.

The second effective factor is HB which was briefly discussed. In the previous section, it was evaluated from bond length analysis that is not a very valid viewpoint (Table 3). Therefore here, the NBO and AIM methodologies were used for examination and certification of HB role in stability (their figures are given in supporting information). The charge transfer energies between involved atoms in HB are displayed in Table 3. The location and strength of HBs were determined for each configuration. The obtained NBO HBs that is resulted from charge transfer positions and their energies are reported in Table 2. Comparison of the bond length analysis and NBO HB numbers show an approximate matching between them.

A more accurate and acceptable tool, AIM calculations, was used for examination the type and position of surface HBs. Topological analysis of five stable configurations are reported in Table 3. The positive values for both of ρ_{BCP} and $\nabla^2\rho_{BCP}$ certificate the existence of HBs on the surface. AIM methodology completely characterized all predicted HBs in the structural analysis section. Numbers and positions of AIM HBs in 4-ethoxy and 3-ethoxy4 surface are identical with NBO analysis but they are different in other forms. The results of Table 3 show that in the 2-ethoxy3, 1-ethoxy2 and 0-ethoxy forms the O_{Sil6} can be contributed as donor atom in new HBs while this does not observe in NBO outcomes (see Table 2). Deep investigation of AIM results displays that there are a good relation between AIM HBs and relative energy. Fig. 8b shows that with increasing the number of AIM HBs the relative energy decreases. This significant outcome approves our guess about the important role of hydrogen bond in the stability order. The more stability of 1-ethoxy2 despite possessing the same number of HBs with 2-ethoxy3 can be explained by the less steric hindrances.

As it was stated in the structural analysis section, in addition of mentioned factors, the existence of HB network on the surface can affect the stability order too. The HB network leads to electron sharing on the system, increasing the available orbitals for electrons and subsequently decreasing the energy level of system. The

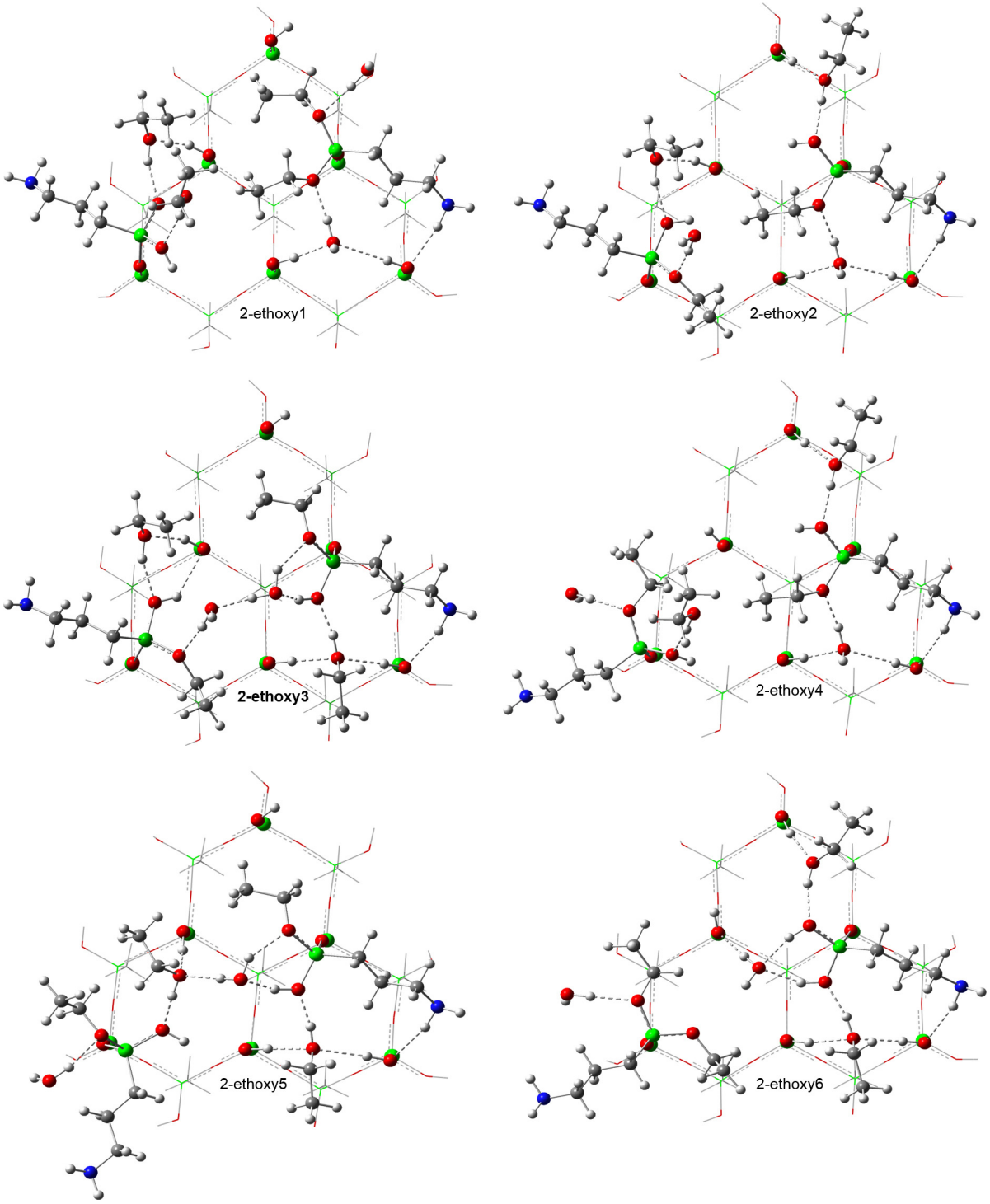

Fig. 5. Optimized structures of 2-ethoxy forms. The HB network in the 2-ethoxy3, 5 and 6 forms is observable.

Table 2
Relative and delocalization energies (kcal mol^{-1}), numbers of HEtO groups, and numbers of HBs from bond length analysis, NBO and AIM methodology.

Category	Relative energy	HEtO	Bond length analysis HB	NBO HB	AIM HB	Electron delocalization energy
4-ethoxy	0	0	7	7	7	968.2
3-ethoxy4	−13.4	1	9	9	9	1003.2
2-ethoxy3	−21.2	2	11	10	11	1003.7
1-ethoxy2	−30.4	3	11	10	11	1042.9
0-ethoxy	−18.6	4	10	9	10	985.2

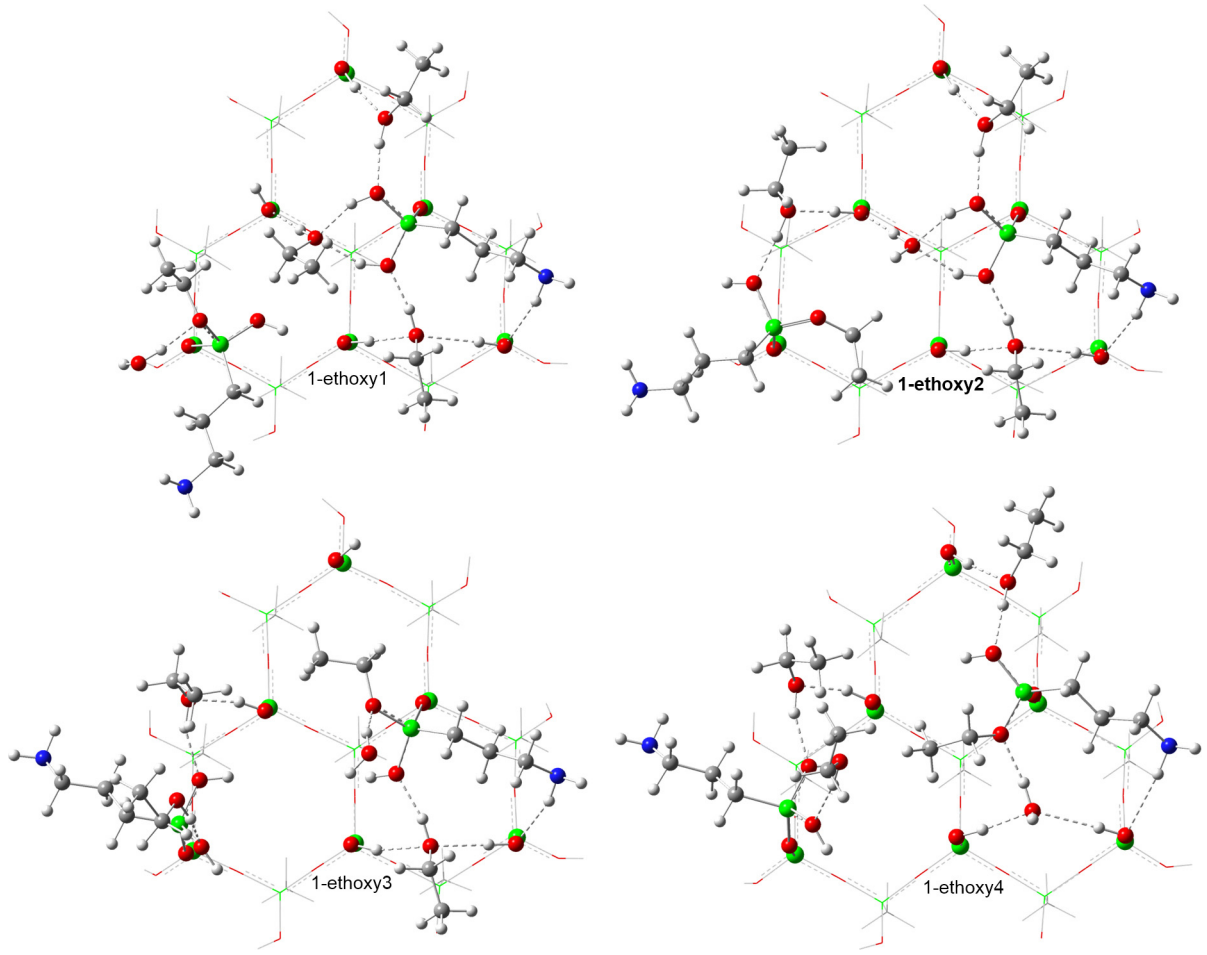

Fig. 6. Configuration structures of 1-ethoxy category that are optimized at the same level. The HB network is obvious in the 1-ethoxy1 and 2 forms.

amount of electron sharing is determined from the electron delocalization energy in NBO results. For five selected configurations, the NBO results were extracted and reported in Table 2. As it is evident, the most stable forms have the most delocalization in their surface. The minimum delocalization is related to 4-ethoxy surface with an unstable form. Therefore, the electron delocalization also like the two other causes plays an important role in stability order.

As a general conclusion based on given all above, it can be inferred that the configuration stability in amino-functionalized silica surfaces is affected by three parameters including the steric hindrance, the numbers of HBs and the electron delocalization

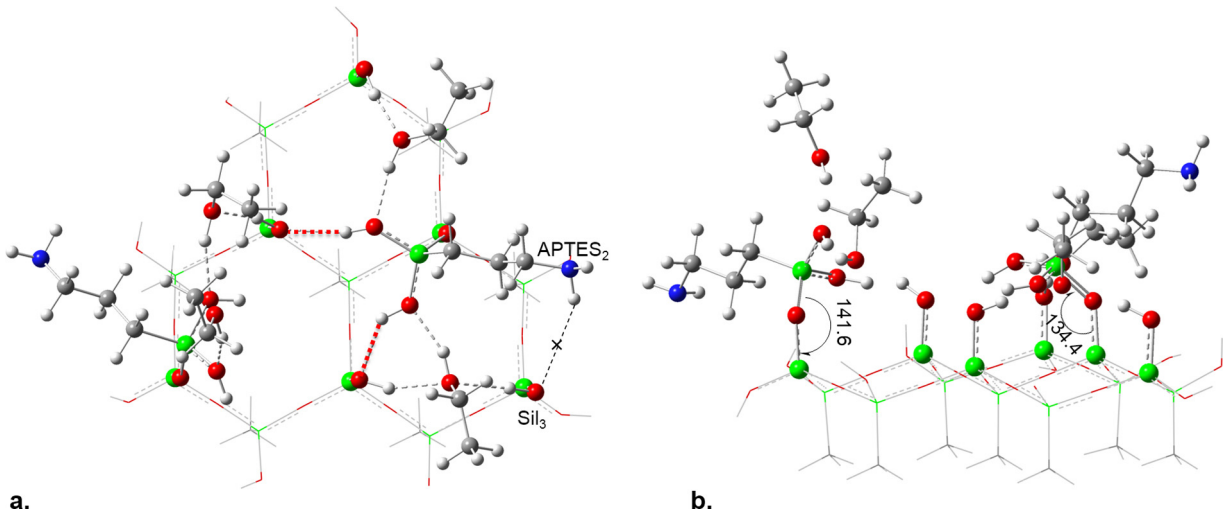

Fig. 7. (a) Two new HBs in the 0-ethoxy form are displayed as red dash lines. (b) Bending of siloxane angles is shown. (For interpretation of the references to color in this figure legend, the reader is referred to the web version of this article.)

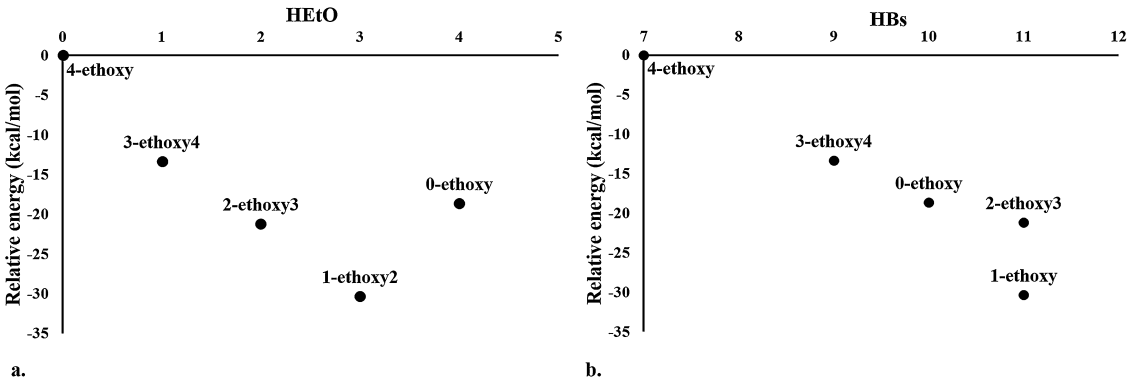

Fig. 8. Relation between relative energy and number of (a) HEtO groups and (b) HBs (from AIM methodology and bond length analysis). Stability increases with increasing of both of them.

Table 3
The calculated HB lengths (Å), charge transfer energies (kcal mol^{-1}) and topological parameters for surface interactions of 4-ethoxy, 3-ethoxy4, 2-ethoxy3, 1-ethoxy2 and 0-ethoxy.

Category	Involved orbitals	Bond length	Charge transfer	Topological parameter	
		O—H	ΔE	ρ_{BCP}	$\nabla^2\rho_{BCP}$
4-ethoxy	LP (O_{OEt1}) → σ* (OH_{W1})	2.0	6.79	0.025	0.088
	LP (O_{OEt2}) → σ* (OH_{W2})	1.9	8.29	0.029	0.104
	LP (O_{OEt3}) → σ* (OH_{W3})	1.9	6.98	0.026	0.094
	LP (O_{1W4}) → σ* (OH_{Sil2})	1.8	14.17	0.032	0.101
	LP (O_{2W4}) → σ* (OH_{Sil3})	2.4	1.08	0.008	0.027
	LP (O_{OEt4}) → σ* (OH_{W4})	1.8	13.26	0.035	0.116
	LP (O_{Sil3}) → σ* (NH_{APTES2})	2.2	1.10	0.014	0.049
3-ethoxy4	LP (O_{OEt1}) → σ* (OH_{W1})	2.0	6.20	0.024	0.085
	LP (O_{OEt2}) → σ* (OH_{W2})	1.8	11.51	0.034	0.119
	LP (O_{W2}) → σ* (OH_{W3})	1.8	16.97	0.038	0.125
	LP (O_{W3}) → σ* (OH_4)	1.6	31.17	0.055	0.143
	LP (O_{OEt3}) → σ* (OH_{W3})	2.1	2.19	0.017	0.063
	LP (O_{OH4}) → σ* (OH_{EtOH4})	1.7	22.50	0.042	0.138
	LP (O_{1EtOH4}) → σ* (OH_{Sil2})	1.9	8.42	0.026	0.081
	LP (O_{2EtOH4}) → σ* (OH_{Sil3})	2.1	3.58	0.019	0.063
	LP (O_{Sil3}) → σ* (NH_{APTES2})	2.3	1.03	0.013	0.044
2-ethoxy3	LP (O_{OH1}) → σ* (OH_{EtOH1})	1.9	9.02	0.028	0.102
	LP (O_{EtOH1}) → σ* (OH_{Sil6})	1.8	16.37	0.038	0.117
	LP (O_{OEt2}) → σ* (OH_{W2})	1.8	12.36	0.034	0.118
	LP (O_{Sil6}) → σ* (OH_1)	2.4	–	0.011	0.036
	LP (O_{W2}) → σ* (OH_{W3})	1.8	16.18	0.036	0.120
	LP (O_{W3}) → σ* (OH_4)	1.6	29.61	0.054	0.142
	LP (O_{OEt3}) → σ* (OH_{W3})	2.1	2.31	0.018	0.064
	LP (O_{OH4}) → σ* (OH_{EtOH4})	1.7	22.62	0.043	0.138
	LP (O_{1EtOH4}) → σ* (OH_{Sil2})	1.9	8.70	0.026	0.083
	LP (O_{2EtOH4}) → σ* (OH_{Sil3})	2.1	5.09	0.019	0.062
	LP (O_{Sil3}) → σ* (NH_{APTES2})	2.3	0.97	0.013	0.044
1-ethoxy2	LP (O_{OH1}) → σ* (OH_{EtOH1})	1.8	13.89	0.034	0.121
	LP (O_{EtOH1}) → σ* (OH_{Sil6})	1.7	25.97	0.051	0.140
	LP (O_{EtOH3}) → σ* (OH_{Sil5})	1.8	13.86	0.033	0.109
	LP (O_{OH3}) → σ* (OH_{EtOH3})	1.9	11.00	0.028	0.097
	LP (O_{Sil6}) → σ* (OH_{W2})	1.7	–	0.047	0.144
	LP (O_{1W2}) → σ* (OH_3)	1.8	12.78	0.034	0.114
	LP (O_{2W2}) → σ* (OH_4)	1.9	10.09	0.029	0.102
	LP (O_{OH4}) → σ* (OH_{EtOH4})	1.8	18.84	0.038	0.130
	LP (O_{1EtOH4}) → σ* (OH_{Sil2})	1.9	11.45	0.031	0.098
	LP (O_{2EtOH4}) → σ* (OH_{Sil3})	2.2	2.93	0.014	0.047
	LP (O_{Sil3}) → σ* (NH_{APTES2})	2.3	0.65	0.011	0.036
0-ethoxy	LP (O_{OH1}) → σ* (OH_{EtOH1})	1.9	8.97	0.027	0.102
	LP (O_{EtOH1}) → σ* (OH_{Sil6})	1.7	22.63	0.048	0.132
	LP (O_{OH2}) → σ* (OH_{EtOH2})	1.9	6.57	0.025	0.097
	LP (O_{Sil6}) → σ* (OH_{OH3})	2.1	–	0.016	0.057
	LP (O_{OH3}) → σ* (OH_{EtOH3})	1.9	9.26	0.026	0.091
	LP (O_{EtOH3}) → σ* (OH_{Sil5})	1.8	17.07	0.038	0.125
	LP (O_{Sil2}) → σ* (OH_{OH4})	2.1	0.61	0.019	0.068
	LP (O_{OH4}) → σ* (OH_{EtOH4})	1.8	13.94	0.034	0.118
	LP (O_{1EtOH4}) → σ* (OH_{Sil2})	1.9	8.24	0.026	0.085
	LP (O_{2EtOH4}) → σ* (OH_{Sil3})	2.1	5.00	0.019	0.062

energy. The 4-ethoxy configuration with maximum steric effects and minimum HBs and electron delocalization energy is the most unstable form. Comparison of other configurations indicates that the domination of two effective parameters leads to configuration stability. Therefore, higher stability of 0-ethoxy with respect to 3-ethoxy 4 arises from the domination of steric hindrance and HB effects than the electron delocalization energy. Similarly, 2-ethoxy 3 is more stable than 0-ethoxy because of its higher HB and electron delocalization energy. However, it seems that the electron delocalization energy and steric effect factors are more effective than HBs number for 1-ethoxy 2 such that with having the less steric hindrance and higher electron delocalization energy is more stable than 2-ethoxy 3.

4. Conclusion

Five categories including 16 configurations of 1 nm^2 amino-functionalized silica surfaces were designed and a DFT: UFF approach has been applied for determination of their stability order. The structural analysis of configurations has shown that the relative energies vary depending on the numbers and positions of hydrolyzed ethoxy groups in attached APTES molecules. The 4-ethoxy and 1-ethoxy 2 with highest and lowest relative energies were the most unstable and stable configurations, respectively. Based on geometrical investigations with hydrolysis of ethoxy groups and decreasing of steric effects, the stability was increased. Moreover, AIM and NBO tools confirmed our prediction about the role of HB in the stability order that can be inferred from bond length analysis. Besides, the electron delocalization on the surface was determined as an effective factor in configurational stability from NBO results. Finally, we reached the conclusion that the stability order was a function of steric effects, HBs numbers and electron delocalization. None of these parameters was individually affected the stability. It means that at least cooperation of two of these factors is required to change the relative energy and determine the configuration stability.

Acknowledgments

The support of Ferdowsi University of Mashhad (Research and technology) for this work (3/21048-07/03/2012) is appreciated. The authors acknowledge from high performance computing center (HPCC) of Ferdowsi university of Mashhad, Iran for their assistances.

Appendix A. Supplementary data

Supplementary data associated with this article can be found, in the online version, at doi:10.1016/j.jmgm.2015.03.006.

References

[1] B. Issa, I. Obaidat, B. Albiss, Y. Haik, Magnetic nanoparticles: surface effects and properties related to biomedicine applications, Int. J. Mol. Sci. 14 (2013) 21266–21305.
[2] S. Abramson, W. Safraou, B. Malezieux, V. Dupuis, S. Borensztajn, E. Briot, et al., An eco-friendly route to magnetic silica microspheres and nanospheres, J. Colloid Interface Sci. 364 (2011) 324–332.
[3] S. Tao, C. Wang, W. Ma, S. Wu, C. Meng, Designed multifunctionalized magnetic mesoporous microsphere for sequential sorption of organic and inorganic pollutants, Microporous Mesoporous Mater. 147 (2012) 295–301.
[4] A.S. Maria Chong, X.S. Zhao, Functionalization of SBA-15 with APTES and characterization of functionalized materials, J. Phys. Chem. B 107 (2003) 12650–12657.
[5] R.M. Pasternack, S. Rivillon Amy, Y.J. Chabal, Attachment of 3-(aminopropyl)triethoxysilane on silicon oxide surfaces: dependence on solution temperature, Langmuir 24 (2008) 12963–12971.
[6] M.C. Burleigh, M.A. Markowitz, M.S. Spector, B.P. Gaber, Direct synthesis of periodic mesoporous organosilicas: functional incorporation by co-condensation with organosilanes, J. Phys. Chem. B 105 (2001) 9935–9942.
[7] M. Zhu, M.Z. Lerum, W. Chen, How to prepare reproducible, homogeneous, and hydrolytically stable aminosilane-derived layers on silica, Langmuir 28 (2012) 416–423.
[8] M.E. Park, J.H. Chang, High throughput human DNA purification with aminosilanes tailored silica-coated magnetic nanoparticles, Mater. Sci. Eng. C 27 (2007) 1232–1235.
[9] K.K. Sharma, A. Anan, R.P. Buckley, W. Ouellette, T. Asefa, Toward efficient nanoporous catalysts: controlling site-isolation and concentration of grafted catalytic sites on nanoporous materials with solvents and colorimetric elucidation of their site-isolation, J. Am. Chem. Soc. 130 (2007) 218–228.
[10] J. Wang, S. Zheng, Y. Shao, J. Liu, Z. Xu, D. Zhu, Amino-functionalized Fe_3O_4@SiO_2 core–shell magnetic nanomaterial as a novel adsorbent for aqueous heavy metals removal, J. Colloid Interface Sci. 349 (2010) 293–299.
[11] E.F. Vansant, P. Voort, K.C. Vrancken, Characterization and Chemical Modification of the Silica Surface, Elsevier, 1995.
[12] H. Ritter, M. Nieminen, M. Karppinen, D. Brühwiler, A comparative study of the functionalization of mesoporous silica MCM-41 by deposition of 3-aminopropyltrimethoxysilane from toluene and from the vapor phase, Microporous Mesoporous Mater. 121 (2009) 79–83.
[13] C.-H. Chiang, N.-I. Liu, J.L. Koenig, Magic-angle cross-polarization carbon 13 NMR study of aminosilane coupling agents on silica surfaces, J. Colloid Interface Sci. 86 (1982) 26–34.
[14] S. Ek, E.I. Iiskola, L. Niinistö, Gas-phase deposition of aminopropylalkoxysilanes on porous silica, Langmuir 19 (2003) 3461–3471.
[15] R.G. Acres, A.V. Ellis, J. Alvino, C.E. Lenahan, D.A. Khodakov, G.F. Metha, et al., Molecular structure of 3-aminopropyltriethoxysilane layers formed on silanol-terminated silicon surfaces, J. Phys. Chem. C 116 (2012) 6289–6297.
[16] J. Kim, P. Seidler, L.S. Wan, C. Fill, Formation, structure, and reactivity of amino-terminated organic films on silicon substrates, J. Colloid Interface Sci. 329 (2009) 114–119.
[17] Y. Deng, Y. Cai, Z. Sun, J. Liu, C. Liu, J. Wei, et al., Multifunctional mesoporous composite microspheres with well-designed nanostructure: a highly integrated catalyst system, J. Am. Chem. Soc. 132 (2010) 8466–8473.
[18] C.Y. Jung, J.S. Kim, H.Y. Kim, J.M. Ha, Y.H. Kim, S.M. Koo, One-pot synthesis and surface modifications of organically modified silica (ORMOSIL) particles having multiple functional groups, J. Colloid Interface Sci. 367 (2012) 67–73.
[19] J.A. Howarter, J.P. Youngblood, Optimization of silica silanization by 3-aminopropyltriethoxysilane, Langmuir 22 (2006) 11142–11147.
[20] I. Roggero, B. Civalleri, P. Ugliengo, Modeling physisorption with the ONIOM method: the case of NH_3 at the isolated hydroxyl group of the silica surface, Chem. Phys. Lett. 341 (2001) 625–632.
[21] The ab initio method, in: Computational Chemistry and Molecular Modeling, Springer, Berlin/Heidelberg, 2008, pp. 155–170.
[22] R.G. Parr, W. Yang, Density-Functional Theory of Atoms and Molecules, Oxford University Press, USA, 1989.
[23] R. Iftimie, P. Minary, M.E. Tuckerman, Ab initio molecular dynamics: concepts, recent developments, and future trends, Proc. Natl. Acad. Sci. U. S. A. 102 (2005) 6654–6659.
[24] S.A. Mian, L.C. Saha, J. Jang, L. Wang, X. Gao, S. Nagase, Density functional theory study of catechol adhesion on silica surfaces, J. Phys. Chem. C 114 (2010) 20793–20800.
[25] S. Dapprich, I. Komáromi, K.S. Byun, K. Morokuma, M.J. Frisch, A new ONIOM implementation in Gaussian98. Part I. The calculation of energies, gradients, vibrational frequencies and electric field derivatives 1 Dedicated to Professor Keiji Morokuma in celebration of his 65th birthday. 1, J. Mol. Struct.-Theochem. 461 (1999) 1–21.
[26] F. Weinhold, C.R. Landis, Natural bond orbitals and extensions of localized bonding concepts, Chem. Educ. Res. Pract. 2 (2001) 91–104.
[27] R. Bader, Atoms in Molecules: A Quantum Theory (International Series of Monographs on Chemistry), Oxford University Press, USA, 1994.
[28] S. Tosoni, B. Civalleri, P. Ugliengo, Hydrophobic behavior of dehydroxylated silica surfaces: a B3LYP periodic study, J. Phys. Chem. C 114 (2010) 19984–19992.
[29] M.J. Stevens, Thoughts on the structure of alkylsilane monolayers, Langmuir 15 (1999) 2773–2778.
[30] S. Ek, A. Root, M. Peussa, L. Niinistö, Determination of the hydroxyl group content in silica by thermogravimetry and a comparison with ^{1}H MAS NMR results, Thermochim. Acta 379 (2001) 201–212.
[31] A.D. Becke, Density-functional thermochemistry. III. The role of exact exchange, J. Chem. Phys. 98 (1993) 5648–5652.
[32] J.P. Perdew, J.A. Chevary, S.H. Vosko, K.A. Jackson, M.R. Pederson, D.J. Singh, et al., Atoms, molecules, solids, and surfaces: applications of the generalized gradient approximation for exchange and correlation, Phys. Rev. B: Condens. Matter 46 (1992) 6671–6687.
[33] G.A. Petersson, A. Bennett, T.G. Tensfeldt, M.A. Al-Laham, W.A. Shirley, J. Mantzaris, A complete basis set model chemistry. I. The total energies of closed-shell atoms and hydrides of the first-row elements, J. Chem. Phys. 89 (1988) 2193–2218.
[34] A.K. Rappe, C.J. Casewit, K.S. Colwell, W.A. Goddard, W.M. Skiff, UFF, a full periodic table force field for molecular mechanics and molecular dynamics simulations, J. Am. Chem. Soc. 114 (1992) 10024–10035.

[35] V. Barone, M. Cossi, J. Tomasi, Geometry optimization of molecular structures in solution by the polarizable continuum model, J. Comput. Chem. 19 (1998) 404–417.
[36] M. Cossi, N. Rega, G. Scalmani, V. Barone, Energies, structures, and electronic properties of molecules in solution with the C-PCM solvation model, J. Comput. Chem. 24 (2003) 669–681.
[37] M.J. Frisch, G.W. Trucks, H.B. Schlegel, G.E. Scuseria, M.A. Robb, J.R. Cheeseman, et al., Gaussian 09, Revision B.01, 2009, Wallingford, CT.
[38] M.S. Sadeghi Googheri, M.R. Housaindokht, H. Sabzyan, Reaction mechanism and free energy profile for acylation of *Candida antarctica* lipase B with methyl-caprylate and acetylcholine: density functional theory calculations, J. Mol. Graph. Model. 54 (2014) 131–140.
[39] E.D. Glendening, A.E. Reed, J.E. Carpenter, F. Weinhold, NBO Version 3.1. (b), J. Comput. Chem. 19 (1998) 628.
[40] T. Keith, AIMAll, Version 10.05.04, TK Gristmill Software, Overland Park KS, USA, 2010.